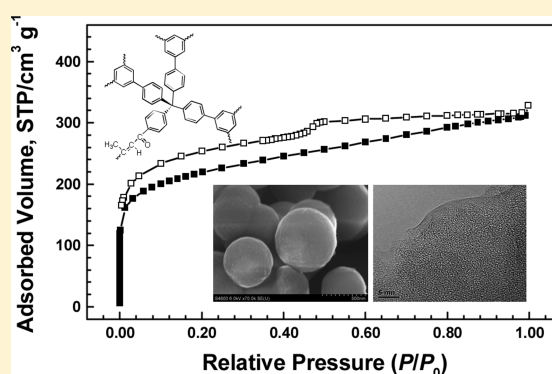


## Thionyl Chloride-Catalyzed Preparation of Microporous Organic Polymers through Aldol Condensation

Yan-Chao Zhao,<sup>†,‡</sup> Ding Zhou,<sup>†</sup> Qi Chen,<sup>†</sup> Xin-Jian Zhang,<sup>†,§</sup> Ning Bian,<sup>†,§</sup> Ai-Di Qi,<sup>§</sup> and Bao-Hang Han<sup>\*,†</sup><sup>†</sup>National Center for Nanoscience and Technology, Beijing 100190, China<sup>‡</sup>Graduate University of Chinese Academy of Sciences, Beijing 100049, China<sup>§</sup>Tianjin Key Laboratory of Modern Chinese Medicine and College of Traditional Chinese Medicine, Tianjin University of Traditional Chinese Medicine, Tianjin 300193, China

S Supporting Information

**ABSTRACT:** We demonstrated the synthesis of five kinds of microporous organic polymers based on aldol self-condensation of di- and multiacetyl-containing building blocks catalyzed by thionyl chloride. The  $\alpha,\beta$ -unsaturated ketone (dimerization) and 1,3,5-trisubstituted benzene (cyclotrimerization) can be observed in the resulting polymers by Fourier transform infrared and solid-state  $^{13}\text{C}$  CP/MAS NMR spectroscopy. The regular spheres and nanometer-scaled cavities were also seen from scanning electron microscopy and high-resolution transmission electron microscopy images. The highest Brunauer–Emmet–Teller specific surface area up to  $832\text{ m}^2\text{ g}^{-1}$  was obtained for the resulting polymers with a pore volume of  $0.48\text{ cm}^3\text{ g}^{-1}$ . The polymers show great hydrogen storage capacities (up to 1.56 wt %) at 77 K and 1 bar. These excellent characteristics would make them become promising candidates for heterogeneous catalysis, separation, and gas storage.



## INTRODUCTION

As a relatively new class of materials, microporous organic polymers containing pores of dimension less than 2.0 nm show great potential applications in areas such as heterogeneous catalysis,<sup>1</sup> separation,<sup>2</sup> and gas storage.<sup>3</sup> Much effort has been made worldwide in the attempt to use new building blocks to assemble various microporous organic polymers over the past decade. These kinds of materials exhibit pronounced advantages against other conventional microporous materials (i.e., zeolites, silica, and activated carbon<sup>4</sup>) and metal–organic frameworks (MOFs).<sup>5</sup> They have modest specific surface area, and the polymers totally composed of the light elements (C, H, O, B, and N) possess quite high gas storage capacity. It is anticipated that by intensive selection of organic building blocks it will be possible to vary the functional groups of the polymers and to introduce specific molecular recognition or catalytic sites.<sup>6,7</sup> Additionally, most of the polymers have desirable resistance to the humid atmosphere even harsh circumstance.<sup>8</sup>

In the early 1970s, hyper-cross-linked polystyrene was first introduced to separate the wastes from polluted water and adsorb organic vapor.<sup>9</sup> On the basis of a multiple Friedel–Crafts alkylation, a series of hyper-cross-linked polymers have been synthesized (such as poly(divinylbenzene-co-vinylbenzyl chloride) resins,<sup>10</sup> poly(chloromethylstyrene)<sup>11</sup>), where extensive cross-linking prevents close packing of polymeric chains. If chosen appropriate building blocks containing nonplanar rigid or contorted site,<sup>12,13</sup> polymers of intrinsic microporosity would be obtained.

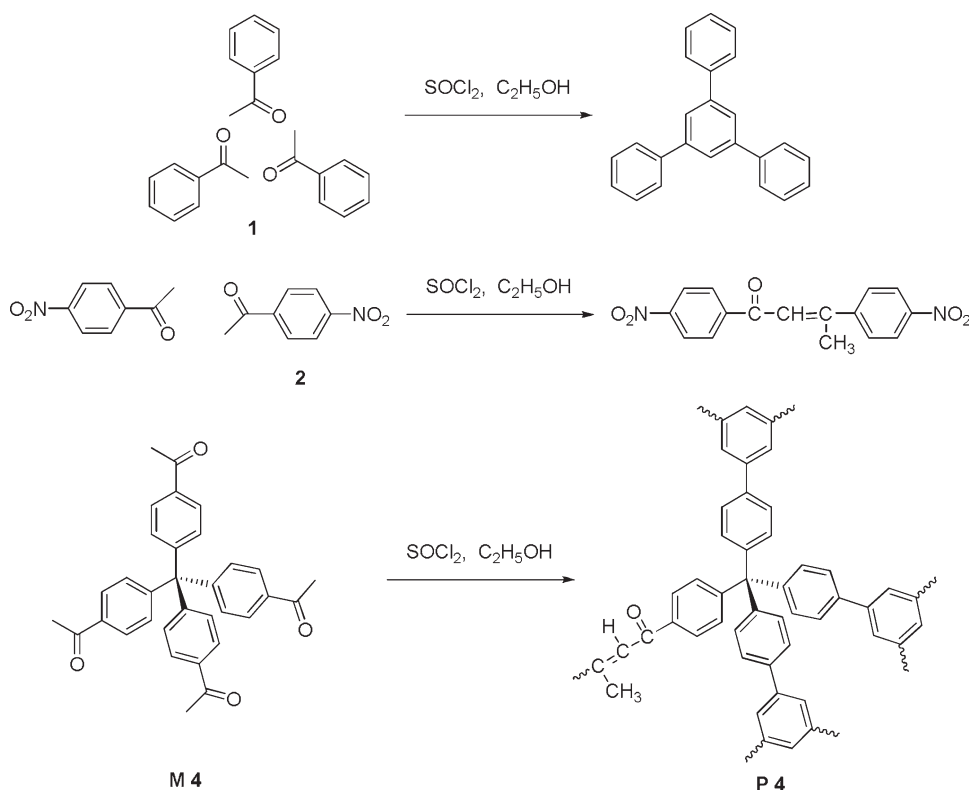
Furthermore, Cu/Pd-mediated ethylalynyl coupling,<sup>14</sup> Pd-mediated Sonogashira–Hagihara<sup>15,16</sup> and Suzuki<sup>17</sup> coupling, Ni(COD)<sub>2</sub>-mediated Yamamoto coupling,<sup>18</sup> FeCl<sub>3</sub>-mediated thiophene–thiophene oxidative coupling,<sup>19</sup> and Co-mediated ethylalynyl cyclotrimerization<sup>19</sup> were extensively employed to synthesize various microporous polymers. Employing the above-mentioned methods, amorphous materials are generally formed under kinetic control. However, covalent organic frameworks (COFs),<sup>20</sup> which are crystalline materials formed by reversible condensation reactions, are different from other microporous materials. They usually possess more uniform pore size and narrow pore size distribution and are linked by reversible covalent bonds such as boroxines and boronates.<sup>21</sup> It has been still a great challenge to tune the porosity of microporous polymers such as specific surface area, micropore volume, pore size, and pore size distribution by varying the monomer strut length and spatial orientation. Meanwhile, it is also an important task to search novel condensation reactions to construct microporous organic polymers in a much easier way.

The aldol (aldehyde–alcohol) condensation is an exceptionally useful atom-economical strategy of C–C bond-forming reaction,<sup>22</sup> in which an active enolate is catalytically generated *in situ* and integrated into the subsequent addition to aldehydes or ketones. The aldol condensation plays a crucial role in the total synthesis of natural products.<sup>23</sup> This kind of reaction was

Received: June 4, 2011

Published: July 18, 2011

**Scheme 1.** Aldol Condensation of Model Compounds **1** and **2** Give Trimeric and Dimeric Products; Condensation of Multitopic **M4** Leads to Three-Dimensional Microporous Polymer **P4**



originally found by the self-condensation of acetaldehyde.  $\beta$ -Hydroxyl aldehyde and  $\beta$ -hydroxyl ketone may eliminate monomolecular water, resulting in the generation of  $\alpha,\beta$ -unsaturated aldehyde and ketone, if stronger acid or base exists in the reaction system.<sup>24</sup> Silicon tetrachloride and thionyl chloride can *in situ* generate hydrogen chloride in the ethanol solution and thus catalyze aldol self-condensation of the acetyl compounds. However, there were few examples of microporous polymers synthesized by aldol condensation routes.<sup>25,26</sup> In this article, we exhibit that a thionyl chloride-catalyzed method is utilized to prepare microporous organic polymers with modest surface area through aldol self-condensation. This facile easily processing procedure is involved with a metal-free method, and the resulting polymers demonstrate ultrahigh hydrogen storage capacities from 0.95 to 1.56 wt % at 77 K and 1 bar.

## EXPERIMENTAL SECTION

**Materials and Methods.** All condensation reactions were operated using the standard Schlenk line technique. Thionyl chloride, acetyl chloride, ferrocene, and biphenyl were purchased from Beijing Chemical Reagent Corp., and thionyl chloride was purified by redistillation. Ferrocene was purified by sublimation prior to use. Anhydrous aluminum chloride was purchased from Aldrich. 1,3,5-Triphenylbenzene, tetraphenylmethane, and 9,9'-spirobifluorene were synthesized according to the reported procedures, respectively.<sup>27–29</sup> Ethanol was purified by refluxing with magnesium powder and trace iodine and then distilled in a nitrogen atmosphere. Dichloromethane, acetone, and other chemical reagents were used as received.

**Preparation of Microporous Organic Polymers.** Two different synthetic approaches (conventional flask method and sealed tube method)

were employed in aldol self-condensation for construction of microporous organic polymers.

**A. Synthesis of Microporous Polymers by Conventional Flask Method.** An acetyl-substituted compound (100 mg, **M1–M5**) was suspended and stirred in beforehand dried ethanol (10.0 mL). At 0 °C, thionyl chloride (1.00 mL) was added gradually to the solution *with caution*, and masses of hydrogen chloride were generated. After 4 h, the temperature was allowed to rise to room temperature, and then the mixture was refluxed for 72 h. The yellow solid was filtrated and washed with acetone, dichloromethane, and ethanol subsequently. The product was dried *in vacuo* at 120 °C for more than 12 h.

**B. Synthesis of Microporous Polymers by Sealed Tube Method.** The di- or multisubstituted acetyl compound (100 mg, **M1–M5**) was suspended in beforehand dried ethanol (4.00 mL). The mixture was degassed by at least three freeze–pump–thaw cycles. To the mixture was added thionyl chloride (1.00 mL) at the temperature of liquid nitrogen. The tube was frozen at 77 K (liquid nitrogen bath) and evacuated to high vacuum and flame-sealed. After 120 °C for 72 h, the reaction mixture gave a yellow solid in a quantitative yield. The yellow solid was filtrated and washed with acetone, dichloromethane, and ethanol subsequently. The product was dried *in vacuo* at 120 °C for more than 12 h.

**Instrumental Characterization.**  $^1\text{H}$  NMR spectra were recorded on a Bruker DMX400 NMR spectrometer, with tetramethylsilane (TMS) as an internal reference. Solid-state  $^{13}\text{C}$  CP/MAS NMR measurements were performed on a Bruker Anence III 400 spectrometer. Thermogravimetric analysis (TGA) was performed on a Pyris Diamond thermogravimetric/differential thermal analyzer by heating the samples at 10 °C  $\text{min}^{-1}$  to 800 °C in the atmosphere of nitrogen. Infrared (IR) spectra were recorded in KBr pellets using a Spectrum One Fourier transform infrared (FT-IR) spectrometer (PerkinElmer Instruments Co. Ltd.). The sample was prepared by dispersing the polymers in KBr

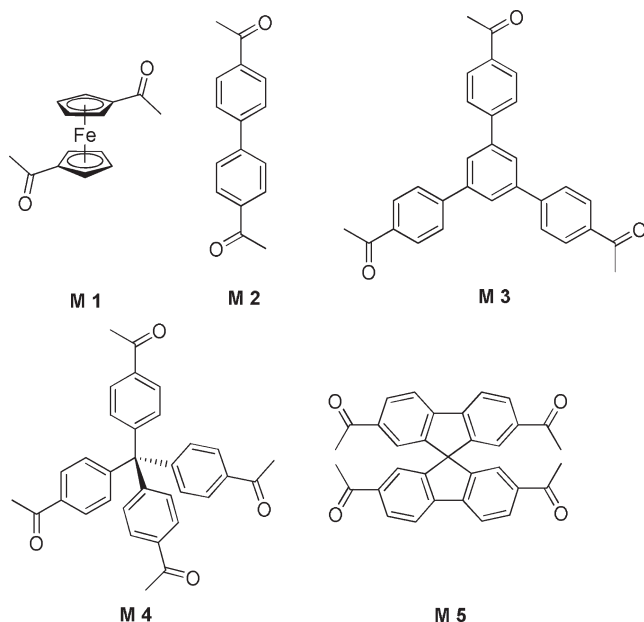


**Figure 1.** Structures of acetyl building blocks (M1–M5) used to prepare microporous polymers (P1–P5).

and compressing the mixtures to form disks, and 15 scans were signal-averaged. High-resolution transmission electron microscopy (HR-TEM) observations were carried out using a Tecnai G<sup>2</sup> F20 U-TWIN microscope (FEI, USA) at an accelerating voltage of 200 kV. Energy dispersive X-ray (EDX) detector was used to analyze the chemical elements of the samples. The sample was prepared by dropping an ethanol suspension of P1–P5 onto a copper grid. Field emission scanning electron microscopy (SEM) observations were performed on a Hitachi S-4800 microscope (Hitachi, Ltd. Japan) operating at an accelerating voltage of 6.0 kV. SEM samples were prepared by dropping an ethanol suspension of P1–P5 on a silicon wafer and then dried. Nitrogen and hydrogen sorption experimentations were conducted using an ASAP 2020 M + C surface area and porosity analyzer (Micromeritics). Before measurement, the samples were degassed *in vacuo* at 120 °C for more than 12 h. Specific surface area was calculated from nitrogen adsorption data by Brunauer–Emmett–Teller (BET) analysis, while pore size and pore size distribution were estimated through the density function theory (DFT). Total pore volume was calculated from nitrogen adsorption–desorption isotherms at  $P/P_0 = 0.97$ .

## RESULTS AND DISCUSSION

The self-condensation of acetophenone results in a new benzene ring formation with elimination of three water molecules.<sup>27</sup> If para-position of the aromatic benzene ring is substituted by an electron-withdrawing group (i.e., nitro), a dimeric product can be obtained (Scheme 1). In order to obtain microporous organic polymers by aldol condensation, various diacetyl (M1 and M2), triacetyl (M3), and tetraacetyl (M4 and M5) building blocks (Figure 1) have been prepared and employed in the one-pot condensation approach. The monomers were suspended and stirred in ethanol via ultrasonication. Thionyl chloride was added gradually to the solution at 0 °C *with caution*. After 1 h, the mixture was heated and refluxed for 72 h, until a series of the yellow monolithic polymers (except P5, see Supporting Information, Figure S1) formed in quantitative yields. The monolith shows no detected crack and scatter after washing with acetone and dichloromethane thoroughly.

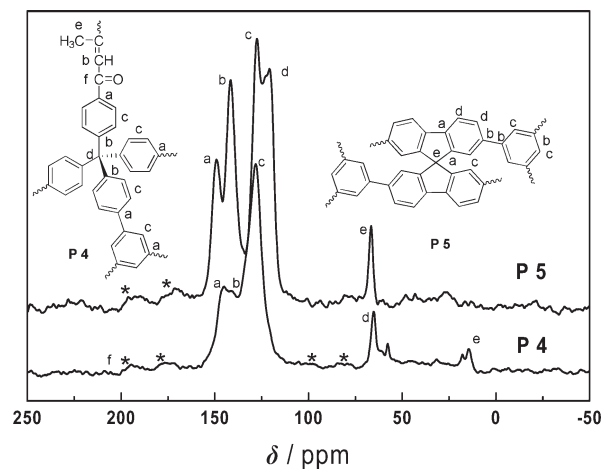


**Figure 2.** Solid-state <sup>13</sup>C CP/MAS NMR spectra of P4 and P5 recorded at MAS rate of 5 kHz. Asterisks (\*) indicate peaks arising from spinning side bands.

Other catalysts were also tested to get high-efficiency condensation products. At first, the self-condensation was tried by using silicon tetrachloride according the reported procedure,<sup>27</sup> in which small triphenylbenzene derivatives were synthesized. The yield of our aldol reaction is much higher than 100%. Silicon dioxide is supposed to incorporate into the skeleton of resulting polymers, resulting in a bicontinuous system. In order to obtain the organic phase, the formed precipitate must be washed with harsh solutions, such as concentrated sodium hydroxide solution or hydrofluoric acid solution. We found that this treatment inevitably damages the organic frameworks to some extent, and there is a small amount of silicon dioxide residue left in the final organic polymers even after careful treatment. However, successful using this procedure to produce organic polymers was reported recently.<sup>26</sup>

Owing to the disadvantage of the silicon tetrachloride/ethanol catalyst, and on account of the nature of acid catalyst of hydrochloride, we tried hydrogen chloride gas as the catalyst, which was generated through dropping concentrated sulfuric acid into hydrochloric acid. However, no polymer could be obtained. Considering the limited concentration of hydrogen chloride gas and open reaction system, the degree of aldol condensation should be much lower, resulting in the failure in the preparation of the porous organic polymers. Finally, thionyl chloride/ethanol was employed in our self-condensation. The thionyl chloride/ethanol catalyst system is a kind of easy-handled catalyst, which is volatile and soluble, and so could be removed from polymers by evaporation and/or Soxhlet extraction with ethanol. We successfully obtained the porous organic polymers using the thionyl chloride/ethanol system.

The self-condensation of various acetyl compounds has been performed in both a conventional flask under an inert gas atmosphere and a sealed tube. In both methods, the reactant solution is treated by freeze–pump–thaw cycles to remove the oxygen and water. As compared to the conventional flask method, the sealed tube method provides an isolated oxygen-free reaction system and anhydrous anaerobic condition. *In situ* generated hydrogen chloride in the ethanol solution cannot leave from the reaction system and can catalyze aldol reaction more efficiently. The absence of water could shift the reaction equilibrium to di- or trimerization of acetyl compounds, and elimination of water is

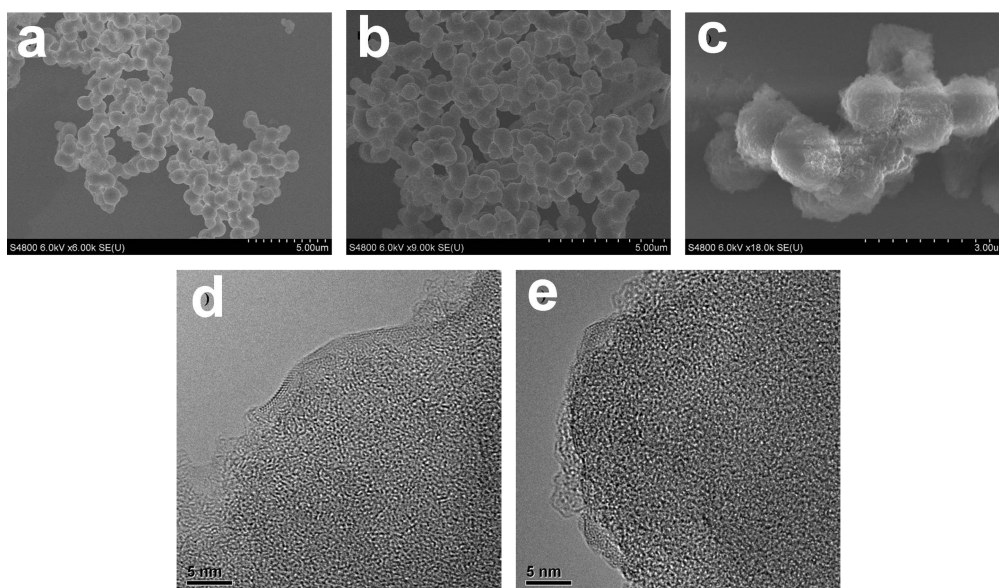


**Figure 3.** SEM images of P4 (a) and P5 (b) synthesized by the conventional flask method and P4 synthesized by the sealed tube method (c); HR-TEM images of P2 (d) and P3 (e).

avored. So a higher degree of self-condensation products might be obtained compared with the conventional flask method.

All the obtained materials show great thermal stability except for P1 demonstrated by thermogravimetric analysis ( $T_{\text{dec}} > 375$  °C, Supporting Information, Figure S2). The polymer P1, which is significantly different from the other polymers, shows one sharp mass lost at 250 °C and residual mass only about 5 wt %. This sharp weight loss can be related to sublimation of cracked ferrocene units. P2 also exhibits a modest weight-loss process, which might be due to a higher conformational flexibility of the biphenyl linker. However, P3, P4, and P5 have higher thermal decomposition temperature and lower mass lost (about 20–30 wt %), which could be explained by the rigid tetrahedral and contorted spiro-center units in the microporous polymers.

The  $\alpha,\beta$ -unsaturated ketone linked polymers were confirmed by FT-IR spectroscopy. In all spectra of the five polymers, bands which can be attributed to the carbonyl stretching of acetyl monomers at 1680–1690  $\text{cm}^{-1}$  are significantly reduced (Supporting Information, Figures S3–S7). Absorption peaks at 1675–1685  $\text{cm}^{-1}$  assigned to the stretching vibration of  $\alpha,\beta$ -unsaturated ketone ( $-\text{C}(\text{O})-\text{C}=\text{C}-$ ) indicate the presence of a dimerization linkage (for the possible reaction mechanism see Figure S8). The characteristic aromatic and aliphatic C–H stretching vibration bands at ca. 3100 and 2900  $\text{cm}^{-1}$  are also observed. Most importantly, P2, P3, and P4 exhibit the diagnostic band at 1500  $\text{cm}^{-1}$  (Supporting Information, Figures S4, S5, and S6) for the 1,3,5-trisubstituted C–C stretching vibration of benzene ring via cyclotrimerization.

A more detailed analysis of the structure of the obtained polymers was performed by solid-state  $^{13}\text{C}$  CP/MAS NMR spectroscopy. Typically, the spectrum of P4 shows five major resonances at 194, ca. 140, 128, 65, and 14 ppm (Figure 2 and Supporting Information, Figure S10). The first one can be assigned to the carbon atoms of carbonyl group, while the signals at ca. 140 and 128 ppm can be ascribed to the carbon of aromatic ring. The possible carbon environments of two kinds of aromatic substituted atoms were also observed at the peak of ca. 140 ppm,

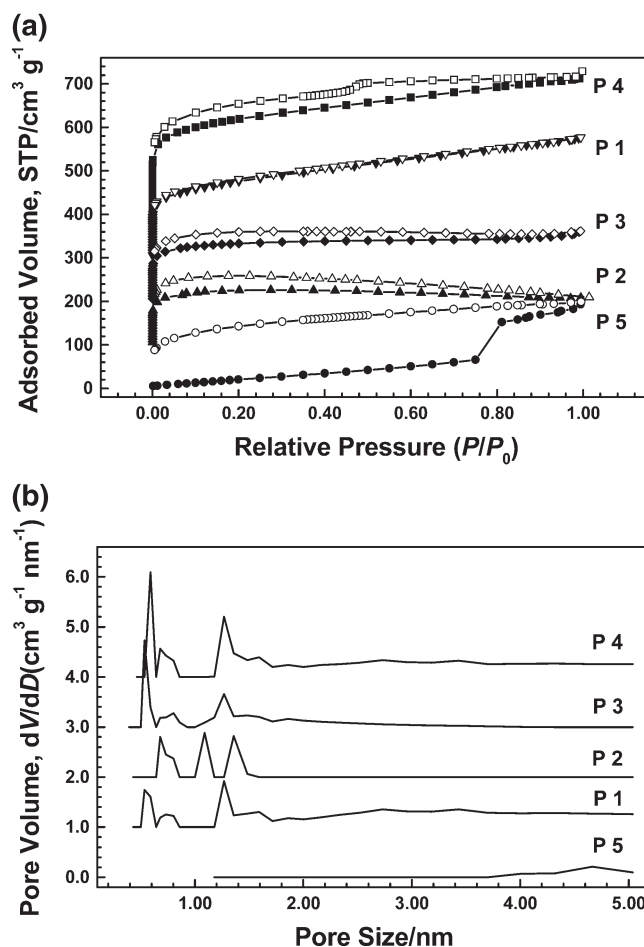


**Figure 4.** (a) Nitrogen adsorption–desorption isotherms of five polymers. The isotherms have been offset by 100 units for the purpose of clarity. (b) Pore size distribution calculated by the DFT method. The curves have been offset by 1 unit for the purpose of clarity.

**Table 1. Porosity Properties and Hydrogen Uptake of Microporous Polymers P1–P5**

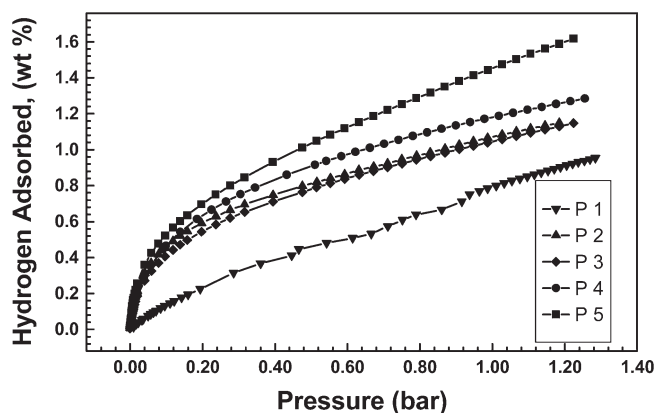
polymers	monomers	$S_{\text{BET}}$ ( $\text{m}^2 \text{g}^{-1}$ ) <sup>a</sup>	$V_{\text{micro}}$ ( $\text{cm}^3 \text{g}^{-1}$ ) <sup>b</sup>	$V_{\text{total}}$ ( $\text{cm}^3 \text{g}^{-1}$ ) <sup>c</sup>	$\text{H}_2$ uptake (%) <sup>d</sup>
P1	M1	616	0.10	0.42	0.95
P2	M2	451	0.16	0.17	1.13
P3	M3	597	0.14	0.24	1.11
P4	M4	832	0.16	0.48	1.25
P5	M5	259	0.00	0.28	1.56

<sup>a</sup> Specific surface area calculated from the nitrogen adsorption isotherm using the BET method. <sup>b</sup> Micropore volume calculated from nitrogen adsorption isotherm using the  $t$ -plot method. <sup>c</sup> Total pore volume at  $P/P_0 = 0.97$ . <sup>d</sup> Hydrogen gravimetric uptake capacities at 77 K measured at hydrogen equilibrium pressure of 1 bar.

which are split into double peaks. The resonance at 65 ppm can be assigned to the quaternary carbon atoms originated from the tetraphenylmethane monomer.<sup>30</sup> The methyl group of  $\alpha,\beta$ -unsaturated ketone in observed at 14 ppm, while 17 ppm may be ascribed to the acetyl end groups. Remarkably, we did not observe these peaks at lower chemical shifts (Supporting Information, Figure S11) in the polymer P5, which suggested a complete self-condensation of the acetyl groups via cyclotrimerization. EDX analysis of all five polymers shows the amount of oxygen element reduced significantly from P1 to P5. The dimerization linkage exists in the skeleton of polymers, where trace oxygen element can be detected. Trace sulfur and chlorine elements which are combined probably into the polymers are also detected in EDX index (Supporting Information, Table S1).

The morphologies of microporous polymers (P1–P5) were investigated by SEM and HR-TEM. The SEM images revealed about 400 nm platelets for P2 and 400–500 nm regular spheres for P4 and P5, whereas no obvious morphology for P3. They display the amorphous and wormlike pores observed from HR-TEM images. For the polymers obtained by the sealed tube method, their surface of nanospheres became more rough (Figure 3 and Supporting Information, Figures S12–S14). Remarkably, the nanometer-scaled cavities can be seen in the edge of polymeric materials from the Figure 3d,e.

Nitrogen adsorption–desorption isotherm measurements can analyze the porous properties of microporous polymers. Figure 4a shows the nitrogen adsorption and desorption isotherms for the resulting polymers. They exhibit typical type I adsorption–desorption isotherms, which show a high gas uptake at very low relative pressures and a flat course in the intermediate section. Using conventional flask procedure, modest Brunauer–Emmet–Teller (BET) specific surface area of  $491 \text{ m}^2 \text{g}^{-1}$  is obtained for P3. Their isotherms display weak hysteresis; the desorption curve lies above the adsorption curve, indicating a swelling efficiency of the polymer matrix<sup>31</sup> or the prevented nitrogen molecules accessible from pores<sup>32</sup> due to the existence of ultramicropores (Supporting Information, Figure S15). For the polymers obtained by the sealed tube method, their hysteresis of the isotherm becomes weaker, indicating a high degree of self-condensation.<sup>6</sup> The porous properties of polymers realize general improvement (Table S2), except for P5. The highest BET specific surface area of  $832 \text{ m}^2 \text{g}^{-1}$  was obtained for P4 with total volume  $0.48 \text{ cm}^3 \text{g}^{-1}$  calculated at  $P/P_0 = 0.97$ , which contains three-dimensional rigid cross-linking tetrahedral units. The surface area of P2 is slightly lower than P1 and P3 due to a

**Figure 5.** Gravimetric hydrogen adsorption isotherms for P1–P5 at 77 K.

higher conformational flexibility of the biphenyl linker.<sup>33</sup> As a contrast, the greatly decreased surface area for P5 may be attributed to a lower reactivity and thermal stability of multi-substituted spirofluorene monomer in sealed glass tube. Figure 4b shows the pore size distribution for the five microporous polymers as calculated using density functional theory (DFT). In the micropore area, three main peaks can be seen in the curves.

The hydrogen adsorption properties of the polymers were also investigated by gravimetric methods (Figure 5). Hydrogen storage capacities for these polymers vary between 1.13 and 1.56 wt % measured at 77 K and 1 bar. Surprisingly, the polymer P5 possesses the highest hydrogen storage capacity up to 1.56 wt %, even though it has a lower surface area. It is anticipated that the resulting polymer contains great amount ultramicropore which can not be accessible by nitrogen.<sup>34</sup> To best of our knowledge, these kinds of materials demonstrate ultrahigh hydrogen storage properties against other microporous polymers with surface area in the range of  $500\text{--}800 \text{ m}^2 \text{g}^{-1}$ . This excellent performance could be due to maximized hydrogen binding energy with a pore size of  $0.70 \text{ nm}$ <sup>35</sup> according to previous simulation results. Similarly, the pore size with  $0.59$  and  $0.67 \text{ nm}$  exists in our types of polymers. Additionally, the polar dimerization linkage has great binding affinity due to dipole–dipole interaction toward hydrogen probably.<sup>36</sup>

## CONCLUSIONS

In summary, we have presented a facile approach to prepare microporous organic polymers through acid-catalyzed aldol condensation. A series of  $\alpha,\beta$ -unsaturated ketone or trisubstituted benzene linked microporous polymers were synthesized, and they all have good thermal stability and modest specific surface area. For the polymers obtained by the sealed tube method, their BET surface areas have been improved markedly, especially for P1 and P4. There are several unique characteristics to make them become the promising materials for potential applications: (1) One-pot condensation approach leads to polymer P4 with BET specific surface area of  $832 \text{ m}^2 \text{g}^{-1}$ . (2) Only cheap single monomers are employed, and they are all easily obtained from Friedel–Crafts acylation reaction. (3) Catalyst and byproduct can remove easily from reaction system, so no heavy metal remains that is evitable in other polymers obtained from organometallic-catalyzed coupling reaction. (4) The polar

dimerization linkage has great binding affinity toward hydrogen, and it also provides a probability of further functionalization. These excellent performances would probably make them become promising candidates for applications. Our further investigations of the gas-selective adsorption and heterogeneous catalysis of these polymers are in progress.

## ■ ASSOCIATED CONTENT

**Supporting Information.** Details of synthetic procedures of monomers, TGA data, FT-IR data, solid-state  $^{13}\text{C}$  CP/MAS NMR spectra, SEM and HR-TEM images, and nitrogen adsorption–desorption data. This material is available free of charge via the Internet at <http://pubs.acs.org>.

## ■ AUTHOR INFORMATION

### Corresponding Author

\*Tel: +86 10 8254 5576. E-mail: [hanbh@nanoctr.cn](mailto:hanbh@nanoctr.cn).

## ■ ACKNOWLEDGMENT

The financial support of the Ministry of Science and Technology of China (National Major Scientific Research Program, Grant 2011CB932500), the National Science Foundation of China (Grants 20972035 and 91023001), and the Chinese Academy of Sciences (Knowledge Innovation Program, Grant KJCX2-YW-H21) is acknowledged.

## ■ REFERENCES

- (1) Hasel, T.; Wood, C. D.; Clowes, R.; Jones, J. T. A.; Khimyak, Y. Z.; Adams, D. J.; Cooper, A. I. Palladium Nanoparticle Incorporation in Conjugated Microporous Polymers by Supercritical Fluid Processing. *Chem. Mater.* **2010**, *22* (2), 557–564.
- (2) McKeown, N. B.; Budd, P. M. Polymers of Intrinsic Microporosity (PIMs): Organic Materials for Membrane Separations, Heterogeneous Catalysis and Hydrogen Storage. *Chem. Soc. Rev.* **2006**, *35* (8), 675–683.
- (3) Morris, R. E.; Wheatley, P. S. Gas Storage in Nanoporous Materials. *Angew. Chem., Int. Ed.* **2008**, *47* (27), 4699–4781.
- (4) Mangun, C. L.; Yue, Z.; Economy, J. Adsorption of Organic Contaminants from Water Using Tailored ACFs. *Chem. Mater.* **2001**, *13* (7), 2356–2360.
- (5) Eddaoudi, M.; Kim, J.; Rosi, N.; Vodak, D.; Wachter, J.; O’Keeffe, M.; Yaghi, O. M. Systematic Design of Pore Size and Functionality in Isoreticular MOFs and Their Application in Methane Storage. *Science* **2002**, *295*, 469–472.
- (6) McKeown, N. B.; Budd, P. M.; Msayib, K. J.; Ghanem, B. S.; Kingstom, H. J.; Tattershall, C. E.; Makhseed, S.; Reynolds, K. J.; Fritsch, D. Polymers of Intrinsic Microporosity (PIMs): Bridging the Void between Microporous and Polymeric Materials. *Chem.–Eur. J.* **2005**, *11* (9), 2610–2620.
- (7) Weder, C. Hole Control in Microporous Polymers. *Angew. Chem., Int. Ed.* **2008**, *47* (3), 448–450.
- (8) Jiang, J.-X.; Su, F.; Trewin, A.; Wood, C. D.; Niu, H.; Jones, J. T. A.; Khimyak, Y. Z.; Cooper, A. I. Synthetic Control of the Pore Dimension and Surface Area in Conjugated Microporous Polymer and Copolymer Networks. *J. Am. Chem. Soc.* **2008**, *130* (24), 7710–7720.
- (9) Tsyurupa, M. P.; Davankov, V. A. Hypercrosslinked Polymers Basic Principle of Preparing The New Class of Polymeric Materials. *React. Funct. Polym.* **2002**, *53* (2–3), 193–203.
- (10) Ahn, J.-H.; Jang, J.-E.; Oh, C.-G.; Ihm, S.-K.; Cortez, J.; Sherrington, D. C. Rapid Generation and Control of Microporosity, Bimodal Pore Size Distribution, and Surface Area in Davankov-Type Hyper-Cross-Linked Resins. *Macromolecules* **2006**, *39* (2), 627–632.
- (11) Lee, J.-Y.; Wood, C. D.; Bradshaw, D.; Rosseinsky, M. J.; Cooper, A. I. Hydrogen Adsorption in Microporous Hypercrosslinked Polymers. *Chem. Commun.* **2006**, *42* (25), 2670–2672.
- (12) McKeown, N. B.; Makhseed, S.; Budd, P. M. Phthalocyanine-based Nanoporous Network Polymers. *Chem. Commun.* **2002**, *38* (23), 2780–2781.
- (13) Mackintosh, H. J.; Budd, P. M.; McKeown, N. B. Catalysis by Microporous Phthalocyanine and Porphyrin Network Polymers. *J. Mater. Chem.* **2008**, *18* (5), 573–578.
- (14) Jiang, J.-X.; Su, F.; Niu, H.; Wood, D. C.; Campbell, N. L.; Khimyak, Y. Z.; Cooper, A. I. Conjugated Microporous Poly(phenylene butadienylylene)s. *Chem. Commun.* **2008**, *44* (4), 486–488.
- (15) Jiang, J.-X.; Su, F.; Trewin, A.; Wood, C. D.; Campbell, N. L.; Niu, H.; Dickinson, C.; Ganin, A. Y.; Rosseinsky, M. J.; Khimyak, Y. Z.; Cooper, A. I. Conjugated Microporous Poly(aryleneethynylene) Networks. *Angew. Chem., Int. Ed.* **2007**, *46* (45), 8574–8578.
- (16) Du, X.; Sun, Y.; Tan, B.; Teng, Q.; Yao, X.; Su, C.; Wang, W. Tröger’s Base-Functionalised Organic Nanoporous Polymer for Heterogeneous Catalysis. *Chem. Commun.* **2010**, *46* (6), 970–972.
- (17) Weber, J.; Thomas, A. Toward Stable Interfaces in Conjugated Polymers Microporous Poly(*p*-phenylene) and Poly(phenyleneethynylene) Based on a Spirobifluorene Building Block. *J. Am. Chem. Soc.* **2008**, *130* (20), 6334–6335.
- (18) Schmidt, J.; Werner, M.; Thomas, A. Conjugated Microporous Polymer Networks via Yamamoto Polymerization. *Macromolecules* **2009**, *42* (13), 4426–4429.
- (19) Yuan, S.; Kirklin, S.; Dorney, B.; Liu, D.-J.; Yu, L. Nanoporous Polymers Containing Stereocontorted Cores for Hydrogen Storage. *Macromolecules* **2009**, *42* (5), 1554–1559.
- (20) Côté, A. P.; Benin, A. I.; Ockwig, N. W.; O’Keeffe, M.; Matzger, A. J.; Yaghi, O. M. Porous, Crystalline, Covalent Organic Frameworks. *Science* **2005**, *310*, 1166–1170.
- (21) El-Kaderi, H. M.; Hunt, J. R.; Mendoza-Cortés, J. L.; Côté, A. P.; Taylor, R. E.; O’Keeffe, M.; Yaghi, O. M. Designed Synthesis of 3D Covalent Organic Frameworks. *Science* **2007**, *316*, 268–272.
- (22) Iwata, M.; Yazaki, R.; Suzuki, Y.; Kumagai, N.; Shibasaki, M. Direct Catalytic Asymmetric Aldol Reactions of Thioamides: Towards a Stereocontrolled Synthesis of 1,3-Polyols. *J. Am. Chem. Soc.* **2009**, *131* (51), 18244–18245.
- (23) Mukherjee, S.; Yang, J. W.; Hoffmann, S.; List, B. Asymmetric Enamine Catalysis. *Chem. Rev.* **2007**, *107* (12), 5471–5569.
- (24) Notz, W.; Tanaka, F.; Barbas, C. F. Enamine-Based Organocatalysis with Proline and Diamines: The Development of Direct Catalytic Asymmetric Aldol, Mannich, Michael, and Diels-Alder Reactions. *Acc. Chem. Res.* **2004**, *37* (8), 580–591.
- (25) Sprick, R. S.; Thomas, A.; Scherf, U. Acid Catalyzed Synthesis of Carbonyl-Functionalized Microporous Ladder Polymers with High Surface Area. *Polym. Chem.* **2010**, *1* (3), 283–285.
- (26) Rose, M.; Klein, N.; Senkovska, I.; Schrage, C.; Wollmann, P.; Böhlmann, W.; Böhlinger, B.; Fichtner, S.; Kaskel, S. A. New Route to Porous Monolithic Organic Frameworks via Cyclotrimerization. *J. Mater. Chem.* **2011**, *21* (3), 711–716.
- (27) Elmorsy, S. S.; Pelter, A.; Smith, K. The Direct Production of Tri- and Hexa-Substituted Benzenes from Ketones under Mild Conditions. *Tetrahedron Lett.* **1991**, *32* (33), 4175–4176.
- (28) Tanemura, K.; Suzuki, T.; Nishida, Y.; Horaguchi, T. Chlorination of Aliphatic Hydrocarbons, Aromatic Compounds, and Olefins in Subcritical Carbon Tetrachloride. *Tetrahedron Lett.* **2008**, *49* (45), 6419–6422.
- (29) Pei, J.; Ni, J.; Zhou, X.-H.; Cao, X.-Y.; Lai, Y.-H. Head-to-Tail Regioregular Oligothiophene-Functionalized 9, 9’-Spirobifluorene Derivatives. I. Synthesis. *J. Org. Chem.* **2002**, *67* (14), 4924–4936.
- (30) Choi, J. H.; Choi, K. M.; Jeon, H. J.; Choi, Y. J.; Lee, Y.; Kang, J. K. Acetylene Gas Mediated Microporous Polymers (ACMPs): First Use of Acetylene Gas as a Building Unit. *Macromolecules* **2010**, *43* (13), 5508–5511.
- (31) Weber, J.; Antonietti, M.; Thomas, A. Microporous Networks of High-Performance Polymers: Elastic Deformations and Gas Sorption Properties. *Macromolecules* **2008**, *41* (8), 2880–2885.

(32) Zhang, B.; Zhang, Z. Building Ultramicropores within Organic Polymers Based on a Thermosetting Cyanate Ester Resin. *Chem. Commun.* **2009**, 45 (33), 5027–5029.

(33) Jiang, J.-X.; Trewin, A.; Su, F.; Wood, C. D.; Niu, H.; Jones, J. T. A.; Khimyak, Y. Z.; Cooper, A. I. Microporous Poly(tri(4-ethynylphenyl)amine) Networks: Synthesis, Properties, and Atomistic Simulation. *Macromolecules* **2009**, 42 (7), 2658–2666.

(34) Germain, J.; Svec, F.; Fréchet, J. M. J. Preparation of Size-Selective Nanoporous Polymer Networks of Aromatic Rings: Potential Adsorbents for Hydrogen Storage. *Chem. Mater.* **2008**, 20 (22), 7069–7076.

(35) Germain, J.; Fréchet, J. M. J.; Svec, F. Nanoporous Polymers for Hydrogen Storage. *Small* **2009**, 5 (10), 1098–1111.

(36) Han, S. S.; Mendoza-Cortés, J. L.; Goddard, W. A. Recent Advances on Simulation and Theory of Hydrogen Storage in Metal–Organic Frameworks and Covalent Organic Frameworks. *Chem. Soc. Rev.* **2009**, 38 (5), 1460–1476.